Journal of Materials Processing Technology 153–154 (2004) 531–536

Journal of Materials Processing Technology

www.elsevier.com/locate/jmatprotec

Fourier thermal analysis of the solidification kinetics in A356/SiC_p cast composites

J.C. Baez [a], C. Gonzalez [a,*], M.R. Chavez [a], M. Castro [b], J. Juarez [a]

[a] *Departamento de Ingenieria Metalurgica, Facultad de Quimica, UNAM, Circuito Exterior S/N, Edif. D, Cd. Universitaria, 04510 Mexico, D.F., Mexico*

[b] *CINVESTAV, Unidad Saltillo, Carretera Saltillo Monterrey Km 13, 25000 Saltillo, Coahuila, Mexico*

Abstract

The aim of this work was to explore the effect of the presence of SiC_p on the solidification kinetics and the microstructural characteristics of A356/SiC_p cast composites by using the Fourier thermal analysis (FTA) method. The tests were performed in order to identify changes in the solidification kinetics of the metal matrix that could be caused by the presence of particle reinforcement. FTA results were complemented with information provided by microstructural characterisation. The outcome of this work suggests that the presence of SiC_p affect the solidification kinetics of both the primary dendritic phase and the eutectic microconstituent. These effects are apparently due to two main causes: (1) the decrease of the latent heat released during solidification associated to the presence of SiC_p and (2) the change in the growth kinetics and morphology of the eutectic present in the metal matrix alloy produced by the nucleation of eutectic Si on SiC_p.

Keywords: Fourier thermal analysis; Metal matrix composites

1. Introduction

Metal matrix composites (MMC) are produced by several processing techniques, and many of the synthesis procedures involve the presence of a liquid alloy in contact with the reinforcement medium [1].

The properties that the composite will show during its work life are intrinsically linked to the nature of the microconstituents present in the solid composite. The microstructural characteristics present in the solidified MMC are determined in turn by the physicochemical interaction within the liquid metal and the reinforcement during processing, and by the kinetics of the phase transformations of the metal matrix, occurring during its solidification and cooling. From this, it is of prime interest to understand the effect of ceramic reinforcement on the solidification kinetics and microstructural characteristics of the metal matrix.

During MMC production, the role of reinforcement particles on the final microstructural characteristics of the composite has not been sufficiently understood. It can be expected that, depending on the nature of the reinforcement particle and the metal matrix, there can be effects on the solidification kinetics (nucleation and growth) of the metal matrix. Also, chemical reactions between particles and metal matrix can produce microconstituents that affects the behaviour of the composite. Finally due to the fact that most of the reinforcement particles do not show phase transformations during composite processing, there is a decrease in the latent heat released during solidification of the composite, compared to the monolithic metal matrix alloy.

It has been found [2] that the presence of silicon carbide particles (SiC_p) reinforcement in Al–Si-based alloys produces a marked difference in the observed thermal analysis parameters between the reinforced and the unreinforced materials. In a previous work [3] it was found that an increase in SiC_p content produces a statistically significant increase in the maximum eutectic temperature during recoalescence, T_{EG}, and a decrease in the local solidification time, t_S. The decrease in t_S was explained as a result of the decrease of the latent heat during solidification as the SiC_p content is increased, such as was indicated by the latent heat data obtained from the numerical processing of the experimental cooling curves by the Newton thermal analysis method. It was suggested that the increase in T_{EG} could be associated with the observed nucleation of eutectic Si on SiC_p. In this regard Braszczynski and Zyska [4] found that the SiC_p accelerate eutectic solidification by the nuclei-forming effect

* Corresponding author. Tel.: +52-55-5622-5225; fax: +52-55-5622-5228.
E-mail addresses: carlosgr@servidor.unam.mx (C. Gonzalez), mcastro@saltillo.cinvestav.mx (M. Castro).

0924-0136/$ – see front matter © 2004 Elsevier B.V. All rights reserved.
doi:10.1016/j.jmatprotec.2004.04.119

of the SiC particles during the solidification of the eutectic silicon. Nucleation on ceramic particles in MMC has been analysed by Kim and Rohatgi [5].

In recent years there have been important advances in the thermal analysis techniques enabling systematic studies on the solidification kinetics of monolithic alloys. The use of these techniques in the study of MMC can contribute to a better understanding of the influence of ceramic reinforcement on the solidification and microstructure of the metal matrix.

The solidification kinetics characterisation of alloys has been addressed by using the method of thermal analysis called Fourier thermal analysis (FTA) [6]. This method is based on the numerical processing of the readings of two thermocouples situated at different radial positions into a cylindrical mold, which contains the melt under study, during its cooling and solidification.

Since this method is based on measurements of the actual thermal field of the liquid metal during solidification, and according with the results obtained from its application to several alloy systems of metallurgical interest [7–10], it is expected to be reliable in its predictions with regards to the solidification kinetic characterisation. The fundamental concepts and implementation, including the considerations that need to be taken into account for its application to the case of MMC, is the subject of the next section.

The purpose of this work was to explore the roll of the presence of SiC_p on the solidification kinetics and microstructural characteristics of the metal matrix A356 alloy by microstructural characterisation and Fourier thermal analysis.

2. Fourier thermal analysis

FTA method assumes that the macroscopic heat flow present in the melt during its cooling and solidification is governed by conductive heat transfer and latent heat generation due to solidification. The energy balance applied to the melt during its solidification can be written as

$$C_v \frac{\partial T}{\partial t} = k\nabla^2 T + L_f \frac{\partial f_S}{\partial t} \tag{1}$$

where C_v (J/m^3 °C) is the volumetric heat capacity, $\partial T/\partial t$ (°C/s) is the rate of change of the temperature of the system as a function of time and k is the thermal conductivity (W/m °C) of the liquid–solid mixture. $\nabla^2 T$ is the temperature Laplacian (°C/m^2), L_f is the volumetric heat of fusion (J/m^3), f_S is the solid fraction and $\partial f_S/\partial t$ is the rate of solid formation. Eq. (1) can be explained in terms of the instantaneous volumetric heat flows (W/m^3) acting during the solidification process of the melt:

$$Q_a = Q_c + Q_S \tag{2}$$

where Q_S is the volumetric heat flow associated with the release of latent heat of solidification, Q_c is the volumetric heat flow exchanged with the surroundings and Q_a is the volumetric heat flow accumulated within the system.

As the major concern of FTA method is the study of solidification, Eq. (1) can be rearranged in terms of Q_S as:

$$Q_S = C_v \left(\frac{\partial T}{\partial t} - \alpha \nabla^2 T \right) = C_v \left(\frac{\partial T}{\partial t} - \mathrm{ZF} \right) \tag{3}$$

where $\alpha = k/C_v$ is the thermal diffusivity of the liquid–solid mixture (m^2/s), and ZF, the Fourier thermal analysis zero curve, is given by the parameter $\alpha\nabla^2 T$.

From Eq. (3), it can be seen that the prevalent volumetric heat flow released as a result of solidification can be found if ZF, $\partial T/\partial t$ and C_v are known.

It has been proposed that in symmetric temperature fields, with respect to the vertical axis of the system (which can be obtained in cylindrical molds thermally isolated at the top and bottom), the temperature Laplacian can be obtained from the readings of two thermocouples, located at R_1 and R_2 distances from the symmetry axis, according to:

$$\nabla^2 T = \frac{4(T_2 - T_1)}{R_2^2 - R_1^2} \tag{4}$$

Furthermore, in the absence of latent heat releasing ($Q_S = 0$), Eq. (3) shows that α, the thermal diffusivity, can be calculated from the temperature Laplacian and the cooling rate data:

$$\alpha = \frac{\partial T/\partial t}{\nabla^2 T} \tag{5}$$

Consequently, when $\partial T/\partial t$ and $\nabla^2 T$ are known before and after solidification, the thermal diffusivities of the liquid, α_L, and the solid, α_S, can be found.

Eq. (3) shows that before and after solidification $\partial T/\partial t$ and ZF are identical. During solidification, the instantaneous value of ZF and C_v of the liquid–solid mixture are calculated as follows:

$$\alpha = \alpha_L(1 - f_S) + \alpha_S f_S \tag{6}$$

$$C_v = C_{v_L}(1 - f_S) + C_{v_S} f_S \tag{7}$$

Using the data provided by Eqs. (6) and (7), the latent heat released by solidification can be calculated according with Eq. (3).

The volumetric latent heat of solidification can be obtained from the integration of Q_S from t_{SS}, the time of start of solidification, to t_{ES}, the time of end of solidification:

$$L_f = \int_{t_{SS}}^{t_{ES}} Q_S \, \mathrm{d}t \tag{8}$$

The instantaneous solid fraction, at time t, can be obtained from

$$f_S = \frac{1}{L_f} \int_{t_{SS}}^{t} Q_S \, \mathrm{d}t \tag{9}$$

Due to the fact that the solid fraction evolution as a function of time is not known at the beginning of the numerical

Table 1
Thermophysical properties of metal matrix and ceramic reinforcement used in this study

Parameter	Description	Magnitude	Reference
ρ_{ML}	Density of liquid A356 alloy	2430 kg/m^3	[10]
ρ_{MS}	Density of solid A356 alloy	2680 kg/m^3	[10]
ρ_p	Density of SiC particles	3200 kg/m^3	[5]
C_{pML}	Heat capacity of liquid A356 alloy	1360 J/kg K	[10]
C_{pMS}	Heat capacity of solid A356 alloy	1211 J/kg K	[10]
C_{pp}	Heat capacity of SiC particles	690 J/kg K	[5]

processing of the cooling curves, a simplified, first approximation of this evolution must be proposed, followed by an iterative procedure.

The numerical processing of the cooling curves involves then, an iterative procedure where, in order to start the iteration, the solid fraction is assumed to be linear with respect to the times of start and end of solidification. Eqs. (6)–(9) are used to calculate the instantaneous ZF, the latent heat released, Q_S, the volumetric latent heat released during solidification of the system, and L_f, the solid fraction evolution as a function of time, and this procedure is iterated until convergence is reached.

It is interesting to note that the only parameter not obtained from the numerical processing of the experimental cooling curves is the volumetric heat capacity of the system during the change of phase.

In order to apply FTA method to the MMC under study, the volumetric heat capacities of interest in this work were calculated by using the data shown in Table 1 and the Eqs. (10) and (11) where f_p is the volume fraction of particle reinforcement

$$C_{v_S} = f_p \rho_p C_{p_p} + (1 - f_P)\rho_{MS} C_{p_{MS}} \quad (10)$$

$$C_{v_L} = f_p \rho_p C_{p_p} + (1 - f_p)\rho_{ML} C_{p_{ML}} \quad (11)$$

3. Experimental procedure

The SiC_p reinforced aluminium alloys were prepared by the melt stirring technique in a clay silicon carbide crucible placed inside a resistance furnace under an argon atmosphere. The SiC_p were mixed into the melt using a pitched-blade turbine impeller driven by a variable speed motor. The metal matrix used in this study was a commercial foundry alloy A356 with the chemical composition shown in Table 2. A Sr master alloy was added in order to achieve a Sr content of 0.015 wt.% in the modified A356 metallic matrix alloy.

Table 2
Chemical composition of the alloy (in wt.%)

Alloy	%Si	%Fe	%Cu	%Mn	%Mg	%Zn	%Al
A356	6.56	0.51	0.12	0.23	0.10	0.06	Balance

Two cases of interest were studied in this work: (1) metal matrix alloy A356, without SiC_p reinforcement; (2) A356/8% SiC_p MMC.

Predetermined quantities of molten composite were poured with minimum turbulence, directly into a sand mould with a cylindrical casting cavity of 0.025 m of internal diameter and 0.15 m in height (with an insulated top and bottom). The pouring temperature was $720 \pm 10\,^{\circ}C$.

In order to record the thermal history of the alloy during cooling, two 0.0003 m diameter bore, type K thermocouples, with alumina sheath, 0.0016 m o.d., were introduced at the mid height of the sand mould cavity at two different distances from the centre of the casting. The thermocouple outputs were recorded by using an Iotech Tempscan 1100 data acquisition system. A calibration procedure [11] was performed with 99.9% aluminium after each experiment.

The solidified rods were cut in halves, in order to verify the positions of the thermocouples and the surfaces were metallographically prepared, and the two sections were used for metallographic analysis.

The experimental SiC_p content was measured by using an image analysis system, indicating for the MMC considered in this work, SiC_p, contents of 7.8 ± 1.2 vol.%. Scanning electron microscopy with electron microprobe analysis was used to identify the different microconstituents in the samples under study. The tests were performed by triplicate.

The cooling curves obtained were numerically processed using the FTA method [7] in order to obtain information about the solidification kinetics of the region of the casting near to the thermocouples.

4. Results and discussion

Fig. 1 shows typical cooling curves associated with the two cases of interest. It can be seen that, as a result of the presence of the SiC_p in the A356 metal matrix alloy, there is a decrease in the local solidification time, which can be inferred from the shortening of the cooling curve corresponding to the composite of interest.

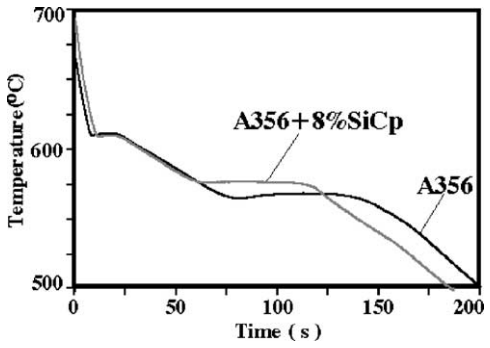

Fig. 1. Cooling curves typically associated with the cases under study.

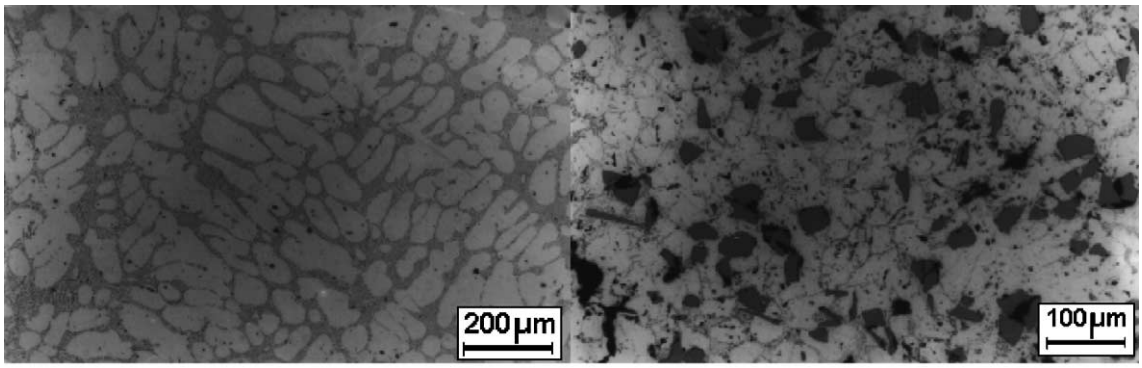

Fig. 2. Microstructures associated with the cases under study.

Another feature that can be readily seen on this figure is the increase of the maximum eutectic undercooling temperature and of the maximum eutectic recoalescence temperature as the SiC_p content is increased.

Fig. 2 shows the microstructures commonly observed in the experimental probes. It can be seen in Fig. 2(a) that unreinforced A356 alloy shows two main microconstituents, the primary phase rich in aluminium, which correspond to the dendritic light gray matrix and the eutectic microconstituent, present as the dark gray, modified Al–Si eutectic at the interdendritic regions. Fig. 2(b) corresponds to the A356/8% SiC_p composite. Here it can be observed that the particles were pushed to the interdendritic and intergranular regions, as it was the case of all the probes containing SiC_p. Particulate reinforcements are generally segregated in the last-freezing zone, as a result of the absence of nucleation of the primary phase on the particle and also, the particles are rejected by the solidifying interfaces (particle pushing phenomena [12]). The absence of nucleation of α-Al on SiC_p in hypoeutectic Al–Si alloys has been explained as a result of the high interfacial energy associated to the aluminium/SiC interface [5].

It can be noted in Fig. 2, the change of morphology of the eutectic microconstituent as a result of the presence of SiC_p. This feature is shown in more detail in Fig. 3(a) and (b) where it can be observed a change in the morphology of the eutectic microconstituent, from modified fibrous in the monolithic A356 alloy, to eutectic lamellar in the case of the MMC under study. This change in morphology and of the associated growth mechanism could explain the measured changes of both the initial nucleation and horizontal parts of the eutectic cooling arrest, which increases as a result of the presence of SiC_p (see Fig. 1).

Fig. 4 shows additional features commonly observed on the experimental composites studied in this work, the nucleation of intermetallic and eutectic microconstituents, on the SiC_p, including the intermetallic $Al_{15}(Fe, Mn)_3Si_2$ (Fig. 3(a)) and the eutectic microconstituent Si (Fig. 3(b)). This evidence probes that ceramic reinforcement in this case shows a physicochemical interaction with the melt which is traduced in effects on the nucleation of microconstituents of the metal matrix.

In order to generate quantitative information on the solidification kinetics of the experimental probes, the Fourier thermal analysis method [7] was applied to the experimental cooling curves.

Fig. 5 shows the latent heat released by unit volume of the cast during solidification as a function of SiC_p content, as revealed by FTA analysis. It can be observed that one of the effects of the presence of reinforcement particles in MMC is, as expected, the decrease of the latent heat released during solidification. This effect in turn enhances the cooling of the

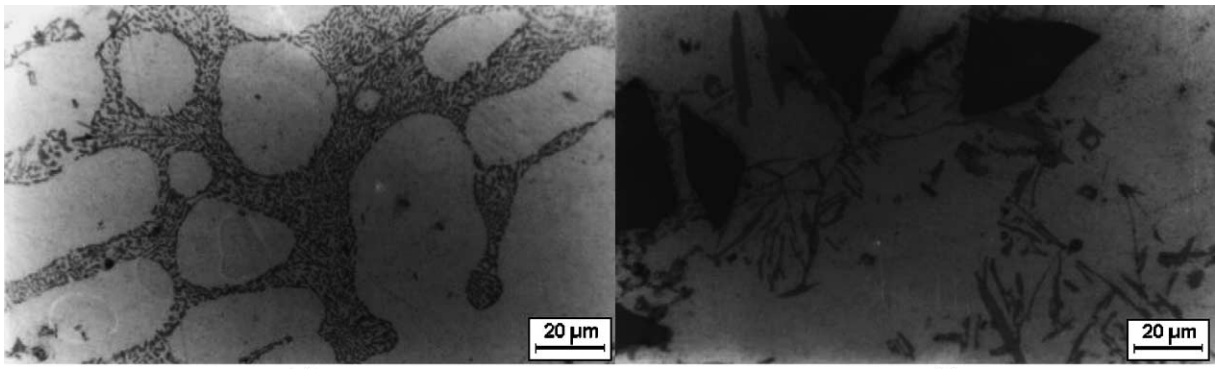

Fig. 3. Eutectic microconstituent morphologies associated with the cases of interest.

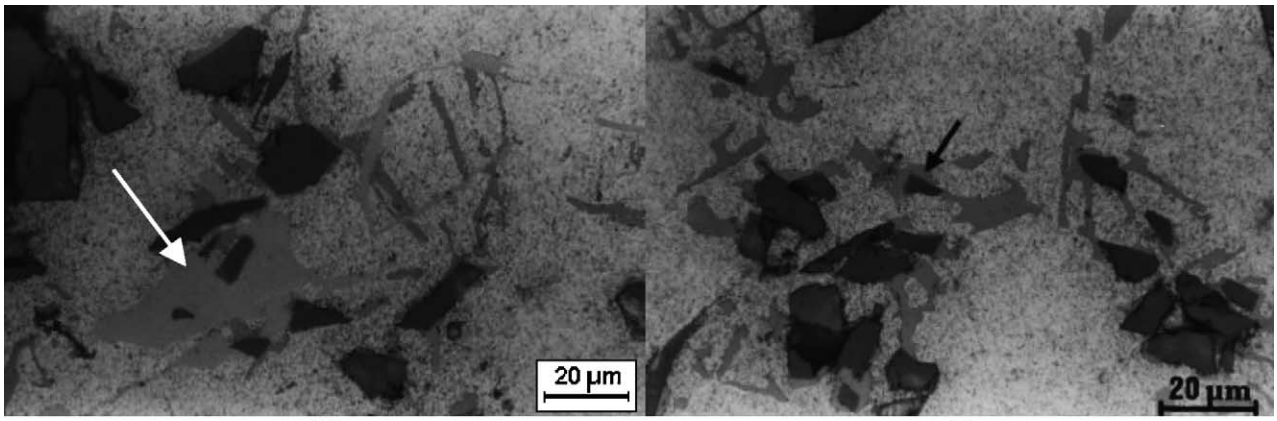

Fig. 4. Nucleation of microconstituents on SiC_p particles in the composite under study.

cast under more severe conditions, and cause the shortening of the cooling curves [3].

The dendritic coherency point is defined as the fraction of solid at which dendrite tips come into contact whit each others all over the casting, forming a solid skeleton and marking the transition from mass feeding to interdendritic feeding.

The temperature difference between the inner and outer thermocouple can be used to evaluate dendrite coherency because, due to the higher thermal conductivity of the solid, the dendritic coherency can be identified from the maximum in ΔT_{ci}, the difference of temperature of the two readings of the thermocouples placed into the casting, plotted against the solid fraction, calculated by FTA, as is shown in Fig. 6 for the cases under study.

It could be expected that the presence of SiC_p has an effect on the average dendritic growth rate, by the increase in the cooling rate associated with the decrease in the latent heat released and also by the interactions between the growing dendrite tips and the particles and the presence of the particle pushing phenomenon, that will locate the particles preferentially in the intergranular and interdendritic regions. From this it can be expected that the coherency solid fraction of the primary phase in the presence of SiC_p will be different from that associated with the monolithic alloy.

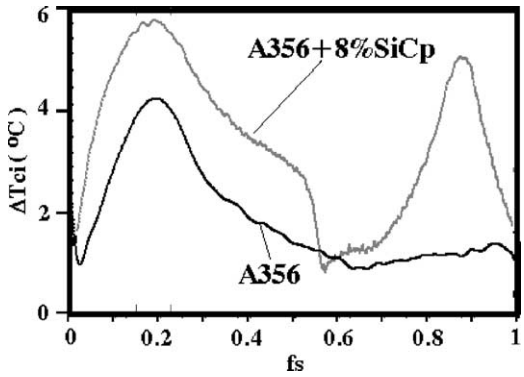

Fig. 6. Dendrite coherency point, as revealed by FTA procedure applied to the cases under study.

Experimental results on dendrite coherency, with a solid fraction at coherency point of 0.19 ± 0.04 for A356 alloy and 0.175 ± 0.03 for the MMC under study shows that there is a trend that indicates the decrease of the solid fraction at the coherency point as a result of the presence of the particles. However the related confidence intervals are overlapped and further work is needed to confirm this trend.

Fig. 7 shows the solidification rate evolution that results from the numerical analysis of the experimental cooling

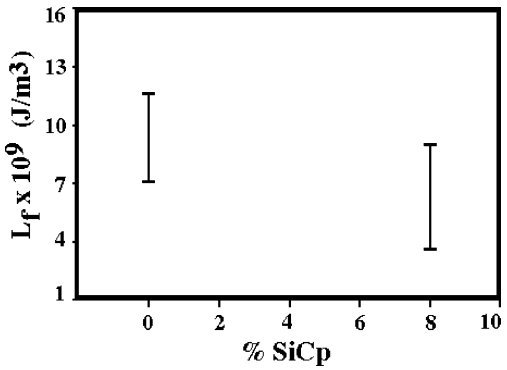

Fig. 5. Latent heat released during solidification as a function of SiC_p content, as revealed by FTA procedure.

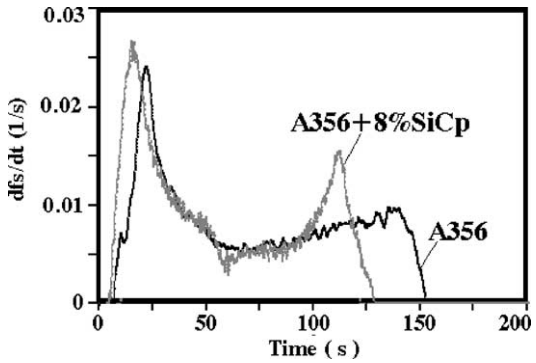

Fig. 7. Solidification rate as a function of SiC_p content, as revealed by FTA procedure applied to the cases under study.

curves for the cases studied in this work, following the FTA procedure. The presence of SiC_p gives place to changes in the solidification kinetics of the dendritic primary phase, as can be seen from the position of the first maximum of the solidification rate associated to each case of interest. This could be a thermal effect caused by an increasing cooling rate with higher SiC_p content that results from the decrease of the latent heat released during solidification [3]. Increasing cooling rates increase the operating undercooling during primary phase solidification which could explain the observed increase in the maximum solidification rate when SiC_p is present.

Fig. 7 shows that the increase in SiC_p content has an important effect on the growth of the eutectic microconstituent. This can be seen from the increase in the second maximum on the solidification rate curves, as the SiC_p content is increased. This effect may be related to the changes in nucleation and growth mechanism of the eutectic microconstituent associated with the presence of SiC_p, as shown by the metallographic findings (see Fig. 3). Apparently, the presence of more nucleation sites for eutectic Si (Fig. 4(b)) gives place to temperature conditions not favourable for the growth of silicon by the induced impurity twin mode and the Si will tend to grow by the twin re-entrant edge mechanism as in unmodified Al–Si eutectic, as can be seen in Fig. 3 where it can be observed that the modification originally present in the eutectic of the metal matrix alloy (Fig. 3(a)) was lost as a result of the presence of SiC_p (Fig. 3(b)). This effect seems to be similar to the poisoning effect of phosphor on the Al–Si eutectic modification with Na and Sr. The AlP acts [13] as an effective heterogeneous nucleating agent of the eutectic Si and produces, as observed for SiC_p in this work, the lost of modification and the increase in the maximum eutectic arrest temperature, T_{EG}. Finally, it is found that the presence of SiC_p, apparently acting as a nucleating agent of eutectic Si, affects the morphology and solidification kinetics of the eutectic present in the metal matrix.

5. Conclusion

The presence of SiC_p changes the solidification kinetics of both the primary dendritic phase and the eutectic microconstituent of the metal matrix.

These effects are apparently due to two main causes: (1) the decrease of the latent heat released during solidification associated to the presence of SiC_p and (2) the change in the growth kinetics and morphology of the eutectic present in the metal matrix alloy produced by the nucleation of eutectic Si on SiC_p.

Acknowledgements

The authors would like to acknowledge DGAPA, UNAM, for the financial support, and S. Garcia, G. Aramburo, A. Amaro, G. González, I. Puente, I. Beltran and C. Atlatenco for their valuable technical assistance.

References

[1] R. Asthana, Review reinforced cast metals. Part 1. Solidification microstructure, J. Mater. Sci. 33 (1998) 1679–1698.
[2] S. Gowri, F.H. Samuel, Effect of cooling rate on the solidification behavior of Al–7 Pct Si–SiC_p metal-matrix composites, Metall. Trans. A 23 (1992) 3369–3375.
[3] C. Gonzalez-Rivera, J. Baez, R. Chavez, A. García, J. Juárez-Islas, Quantification of the SiC_p content in molten Al-Si/SiC_p composites by computer aided thermal analysis, J. Mater. Process. Technol. 143–144 (2003) 860–865.
[4] J. Braszczynski, A. Zyska, Analysis of the influence of ceramic particles on the solidification process of metal matrix composites, Mater. Sci. Eng. A 278 (2000) 195–203.
[5] J.K. Kim, P.K. Rohatgi, Nucleation on ceramic particles in cast metal-matrix composites, Metall. Mater. Trans. A 31 (2000) 1295–1304.
[6] E. Fras, W. Kapturkiewicz, A new concept in thermal analysis of castings, AFS Trans. 101 (1993) 505–511.
[7] E. Fras, W. Kapturkiewicz, A. Burbielko, H.F. Lopez, Numerical simulation and Fourier thermal analysis of the solidification kinetics in high-carbon Fe–C alloys, Metall. Mater. Trans. B 28 (1997) 115–123.
[8] C. González Rivera, B. Campillo, M. Castro, M. Herrera, J. Juarez Islas, On the local microstructural characteristics observed in sand cast Al–Si alloys, Mater. Sci. Eng. A 279 (2000) 149–159.
[9] D. Emadi, L.V. Whiting, Determination of solidification characteristics of Al–Si alloys by thermal analysis, AFS Trans. 110 (2002) 285–296.
[10] M.B. Djurdjevic, W. Kasprzak, A. Kierkus, W.T. Kierkus, J.H. Sokolowski, Quantification of Cu enriched phases in synthetic 3XX aluminium alloys using the thermal analysis technique, AFS Trans. 109 (2001) 517–528.
[11] D. Sparkman, A. Kearney, Breakthrough in aluminum alloy thermal analysis technology for process control, AFS Trans. 102 (1994) 455–460.
[12] J.K. Kim, P.K. Rohatgi, The Effect of the diffusion of solute between the particle and the interface on the particle pushing phenomena, Acta Mater. 46 (1998) 1115–1123.
[13] J.H. Kim, I.S. Kwon, K.M. Kim, C.H. Lee, E.P. Yoon, Effect of phosphorus on modification of eutectic silicon in Al–7Si–0.3Mg alloy, Mater. Sci. Technol. 16 (2000) 243–248.